Supporting Information

Karmakar and Parisi 10.1073/pnas.1222848110

SI Materials and Methods

Criterion for Pinning Random Particles. We equilibrate the system at reduced temperature $T = 1.00$, which is quite high in this case. After equilibrating these configurations, we randomly choose the pinning particles and freeze them in space and time. Then, we decrease the temperature to the required temperature and equilibrate it. So, in short, the particles are frozen from the high-temperature configuration. This is done for the simple reason that at lower temperatures, the unconstrained system crystallizes; therefore, if we do not freeze the particles at high temperature, we will not be able to suppress the crystallization. It is important to note that in ref. 1, the particles are frozen starting from the equilibrium configuration at the required temperature, which differs from our protocol. It remains to be seen whether these different protocols lead to different qualitative results. We expect that the results might be different in general for these two cases, as the nature of the disorder changes quantitatively. We also expect that the choice of temperature at which we equilibrate the particles before freezing should be crucial as it is in the high-temperature phase, as discussed in ref. 2.

Time–Temperature Superposition for $Q(t)$. In Fig. S1, we show the time–temperature superposition for the full overlap correlation function $Q(t)$ with the same relaxation time τ_α used to collapse the data for the self part of the correlation function, i.e., $Q_s(t)$. The figure clearly shows that initial decay of the correlation function is the same as that of the self part only. $Q(t)$ deviates from the master curve because of the nonzero asymptotic value $Q(\infty)$. In this figure, we also plot the data for all system sizes. Different colors indicate the temperatures, and the symbols distinguish the different system sizes. The inset shows the temperature dependence of the asymptotic value of $Q(t)$, i.e., $Q(\infty)$, and one can see clearly that there are very small finite size effects in this quantity.

Extraction of Static Length Scale from the Replica Correlation Function. As discussed in *Materials and Methods* in the main article about how we extracted the length scale from the replica correlation function, we present here some data for the $N = 4{,}000$ system size in Fig. S2. We used the method explained in *Materials and Methods*,*Replica Overlap and Extraction of Static Length Scale* . The nice fitting of the data over the whole range and for all temperatures indicates that the extracted length scale is very reliable. This also can be seen from the data shown in Fig. 1, in which we compare the results of this fitting for different system sizes. The data for $N = 2{,}000$ is very close to the one obtained from the $N = 4{,}000$ system size. This implies that this method of extraction of the length scale is very robust once we rule out the finite size effect in the data.

Parallel Tempering Methods. To equilibrate the system at an even lower temperature, we have implemented the parallel tempering method. We mention this method here only briefly, as details may be found in ref. 3. We construct a system consisting of M noninteracting subsystems (replicas), each consisting of N particles with phase space coordinate $\{P^i, Q^i\}$, where $P^i = \{p_1, p_2 \ldots p_N\}$ and $Q^i = \{q_1, q_2, \ldots q_N\}$ for the i^{th} subsystem. The Hamiltonian of the i^{th} subsystem is given by

$$H_i(P^i, Q^i) = K(P^i) + \Lambda_i E(Q^i), \qquad \text{[S1]}$$

where K is the kinetic energy, E is the potential energy of the system, and $\Lambda_i \in \{\lambda_1, \ldots \lambda_M\}$ is the parameter to rescale the potential energy. Next, we perform a molecular dynamics (MD) simulation of the whole system with Hamiltonian $\mathcal{H} = \sum_i^M H_i$ at a reduced temperature $T = 1/\beta_0$ using a modified isokinetic simulation method. The time step for the MD is taken to be $\delta t = 0.005$. Then, at each time interval of $\Delta t_X = 1{,}000\delta t$ we exchange the parameter λ between different replica i and j, keeping all other things unchanged. The exchange is accepted using a Metropolis scheme, with a probability

$$w_{i,j} = \min\left(1, \exp\left(-\Delta_{i,j}\right)\right), \text{ where } \Delta_{i,j} = \beta_0\left(\Lambda_j - \Lambda_i\right)\left(E\left(Q^i\right) - E\left(Q^j\right)\right). \qquad \text{[S2]}$$

We perform these steps long enough get proper equilibration of the system; this way, we generate canonical distribution at inverse temperatures $\beta = \lambda_i\beta_0$. Here, we also parallelized the code using message passing interface to speed the simulation process. We used $M = 12$ replicas between temperatures 0.300 and 0.600 and another 12 replicas for temperature range 0.600–1.000 for $N = 100$ and 150 system sizes. For $N = 200$, we used 16 replicas for the 0.300–0.600 temperature range and 12 between 0.600 and 1.000. For $N = 250$, we tried to equilibrate the system only up to $T = 0.330$ and used 16 replicas between temperatures 0.330 and 0.600 and 12 between 0.600 and 1.000. We averaged the data over 400 different realizations of the disorder for systems $N = 100$, 150, 200, and 250. Therefore, the estimated computer time for the $N = 250$ system size is close to 10^5 h. To check the equilibration of the system, we used the method in ref. 3 to rescale the canonical distribution function using the formula

$$P_i(E; T_j = \lambda_j\beta_0) = \frac{P_i(E)\exp\left[\left(\lambda_i - \lambda_j\right)\beta_0 E\right]}{\int dE' P_i(E')\exp\left[\left(\lambda_i - \lambda_j\right)\beta_0 E'\right]}. \qquad \text{[S3]}$$

In equilibrium, the left-hand side of the above equation should be independent of i to within the accuracy of the data, as may be seen in Fig. 2 *Left*.

Check of Equilibration in Parallel Tempering Runs. We performed two separate tests to check the equilibration of our sample. One was a test of the distribution of energy $P(E)$, in which we tried to rescale all the $P(E)$ for different temperatures to collapse on the distribution of our reference temperature T_0 as shown in Fig. 2 in the main article using the ansatz Eq. S3. Here we present the data for the second test, which determined when the square of the replica overlap $\langle q^2 \rangle$ reached a steady plateau value with time. In Fig. S3, we show data for the $N = 100$ system size, and the data clearly show that our simulation time is longer than the time required to reach a plateau value for $\langle q^2 \rangle$. Because we started from two completely uncorrelated replicas, their initial overlap is very small and over time reaches the equilibrium value from below.

Fig. S4 shows the spin glass susceptibility χ calculated for all four system sizes for two different run lengths. Run1 is 1×10^8 MD steps long, and Run2 is two times longer than Run1. The value of the susceptibility is within the error bar of each other, which also confirms that our data are well equilibrated.

Sample-to-Sample Variation of $P(q)$. In this section, we show the sample-to-sample fluctuations of the distribution of $P(q)$ for two different system sizes at the lowest temperature simulated for two system sizes $N = 150$ and 250. Fig. S5 shows $P(q)$ for eight randomly chosen samples. One can see clearly the strong sample-to-sample fluctuations of this distribution, which also is very similar to

spin glass models (4). Some samples have only two peaks, with a deep valley between them, whereas others have a third peak.

Skewness and Kurtosis. In Fig. S6, we show the skewness (S) and the kurtosis (B), defined as

$$S = \frac{[\langle \delta q^3 \rangle]}{[\langle \delta q^2 \rangle]^{3/2}}, \quad B = 3.0 - \frac{[\langle \delta q^4 \rangle]}{[\langle \delta q^2 \rangle]^2} \quad \text{with} \quad \delta q = q - \langle q \rangle. \quad \textbf{[S4]}$$

The usual Binder cumulant is equal to $g(T) = B/2.0$ according to our definition. Notice that $g(T)$ is a nonmonotonic function of temperature. In conventional phase transition, this is a very useful quantity that has been used extensively in finite size-scaling analysis for determining the critical temperature in the thermodynamic limit. These quantities for different system sizes cross each other at critical temperature because of the finite size scaling.

At zero magnetic field in the Sherrington–Kirkpatrick model for spin glass and the short-range Edwards–Anderson model, $g(T)$ is always a positive function of T and increases regularly with decreasing temperature and the skewness is identically zero. Unfortunately, as soon as the magnetic field differs from zero in the Sherrington–Kirkpatrick model (in which mean field theory is correct), the behavior at the transition point for the cumulant is much more complex, and for 1,024 spins, we also are very far from the asymptotic limit (5).

The behavior we see here is distinctly different from this simple case. Moreover, it is nonmonotonic and mostly a negative function of temperature over almost the whole range. This stems from the fact that the distribution of q, $P(q)$ starts to become non-Gaussian at quite a high temperature. This behavior is similar to that seen for the finite-range three-spin model in four dimensions (6), in which the skewness decreases strongly toward the large negative values when the temperature decreases. This similarity once again seems to suggest that this model also may be in the same universality class as short-range three-spin glasses, which apparently have their own universality class. We need further study to clearly determine the exact nature of the transition, if any.

1. Cammarota C, Biroli G (2012) Ideal glass transitions by random pinning. *Proc Natl Acad Sci USA* 109(23):8850–8855.
2. Cammarota C (2012) A general approach to systems with randomly pinned particles: Unfolding and clarifying the random pinning glass transition. arXiv:1211.4001v1.
3. Yamamoto R, Kob W (2000) Replica-exchange molecular dynamics simulation for supercooled liquids. *Phys Rev E Stat Phys Plasmas Fluids Relat Interdiscip Topics* 61(5B): 5473–5476.
4. Parisi G, Ricci-Tersenghi F (2012) A numerical study of the overlap probability distribution and its sample-to-sample fluctuations in a mean-field model. *Philos Mag B* 92:341.
5. Billoire A, Coluzzi B (2003) Numerical study of the SK model in magnetic field. *Phys Rev E Stat Nonlin Soft Matter Phys* 68:026131.
6. Parisi G, Picco M, Ritort F (1999) Continuous phase transition in a spin-glass model without time-reversal symmetry. *Phys Rev E Stat Phys Plasmas Fluids Relat Interdiscip Topics* 60(1):58–68.

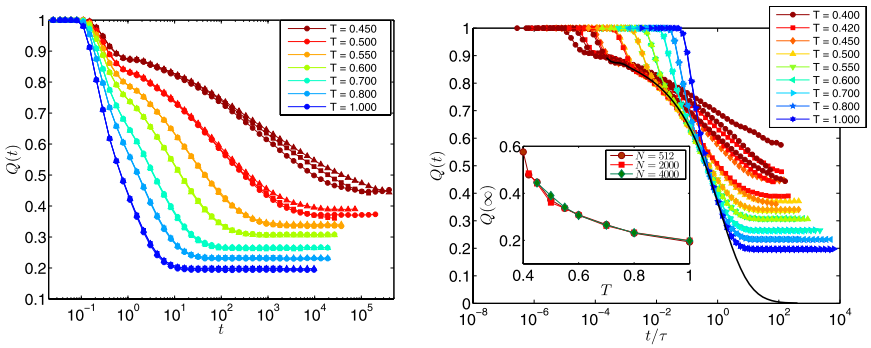

Fig. S1. Data for $N = 512$, $N = 2{,}000$, and $N = 4{,}000$. (*Left*) System size dependence of the relaxation function $Q(t)$. One can see that there is a very small finite size effect in these system sizes. (*Right*) Time–temperature superposition of $Q(t)$ using the relaxation time τ_α obtained from the self part of $Q(t)$ from the condition $Q_s(\tau_\alpha) = 1/e$. It clearly shows that the initial part of the relaxation function is very much the same as that of the self part but deviates from it, as the infinite time value of $Q(t)$ is not 0 in this case. The black solid line is the master curve obtained if one tried to do the time–temperature superposition for $Q_s(t)$ as done in Fig. 1. This is shown just to point out that the master curve for $Q(t)$ also follows the same curve but deviates from it because of the nonzero asymptotic value. (*Inset*) Temperature dependence of the infinite time value of $Q(t)$ that is $Q(\infty)$ for all system sizes. One clearly can see that there is hardly any system size dependence in this quantity.

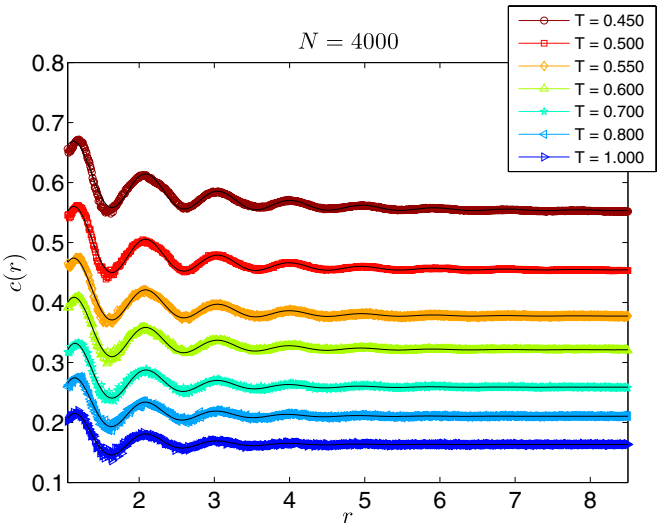

Fig. S2. Extraction of the static length scale for $N = 4{,}000$ system size. We used the functional form $\tilde{c}(x) = a + \exp(-x/\xi)[b + c\cos(xd + e)]$ to fit the data. The nice fitting over the whole range of the data indicates that the length scale extracted this way is very reliable. Data for different curves are shifted vertically by 0.01 from each curve for clarity.

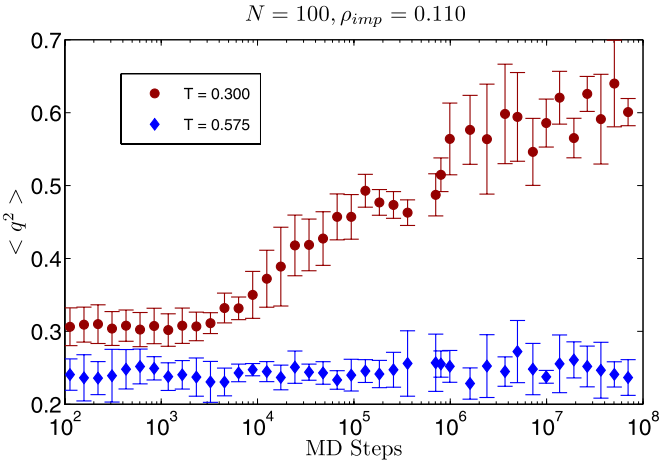

Fig. S3. Evolution of $\langle q^2 \rangle$ as a function of MD steps to check whether the time evolution of $\langle q^2 \rangle$ reached a plateau. We take the sample to be equilibrated if $\langle q^2 \rangle$ reaches a plateau value within the error bar.

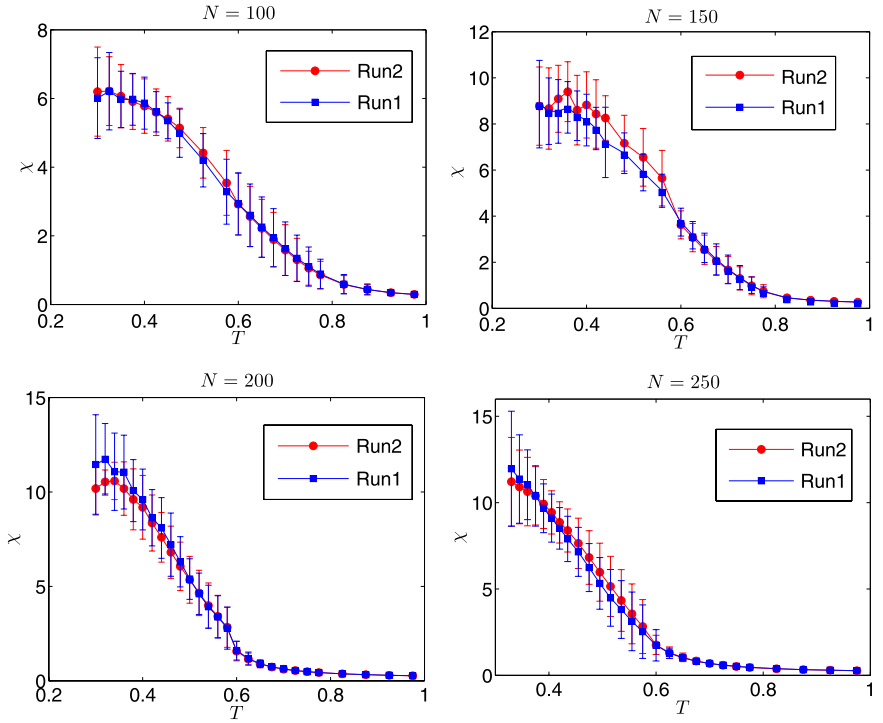

Fig. S4. Comparison of susceptibility χ for two sets of runs for different system sizes. Run2 is two times longer than Run1. Error bars are calculated by the bootstrap method.

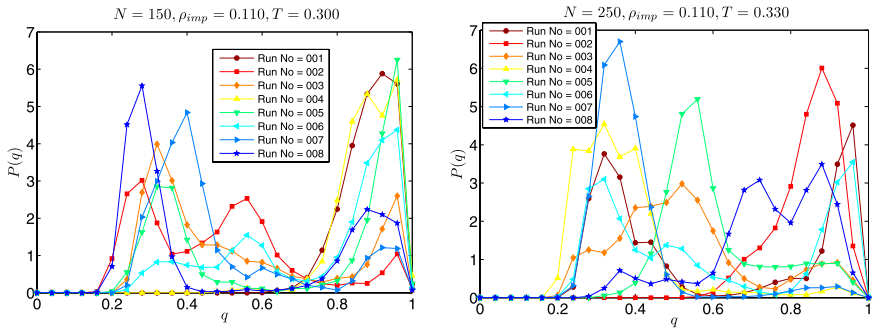

Fig. S5. (*Left*) Distribution of overlap $P(q)$ for $N = 150$ system size with $\rho_{imp} = 0.110$ for the temperature $T = 0.300$ for eight different samples. (*Right*) Distribution for the $N = 250$ system size at $T = 0.330$.

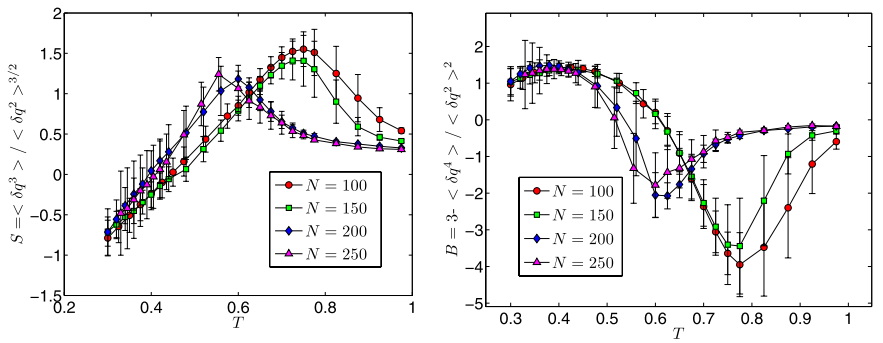

Fig. S6. (*Left*) Temperature dependence of skewness S for different system sizes with $\rho_{imp} = 0.110$. (*Right*) Kurtosis for the same dataset.